



Adsorption and Thermodynamic Studies of Watermelon Seed Ethanol Extract on the Corrosion Inhibition of Zinc in Nitric Acid

^{1,2*} Aliyu, M. and ¹Ibrahim, M. B.

¹Department of Pure and Industrial Chemistry, Bayero University, Kano P.M.B. 3011, BUK, Kano, Nigeria

²Department of Pure and Applied Chemistry, Usmanu Danfodiyo University, P.M.B. 2346, Sokoto, Nigeria

*Correspondence Email: musa.aliyu1@udusok.edu.ng

ABSTRACT

The corrosion inhibition potentials of ethanol extracts of watermelon seed (WSE) was investigated. The inhibition properties were investigated using weight loss measurement; Fourier transforms infrared (FT-IR) spectroscopy and scanning electron microscopy (SEM). The results obtained showed that the corrosion inhibition efficiency increases with increase in the concentration of the WSE. 0.10 % v/v concentration of WSE showed a maximum corrosion inhibition efficiency of 42.4551 % at 28±1 °C. The adsorption data were modeled with Langmuir, Freundlich, Frumkin, Temkin and Flory-Huggins isotherm models with the Langmuir isotherm having the best fit (R^2 0.998 – 0.999). It was more fitted to Freundlich isotherm. The adsorption process indicated feasible and spontaneous process from the large negative values of ΔG_{ads} . The values of ΔH_{ads} are all negative indicating exothermic process of adsorption. The results of FT-IR spectra showed that the inhibitor compounds were adsorbed on the zinc surface. The SEM micrographs result showed the formation of adsorbed inhibitor compounds on the zinc surface. The WSE was found to be effective and reduced the corrosion rate of zinc in nitric acid.

Keywords: Adsorption isotherms, Corrosion, Inhibition, Watermelon seed, Weight loss, Zinc

INTRODUCTION

The importance of zinc cannot be repudiated in the building constructions, electrical fittings and chemical industries based on their cost effectiveness and tremendous electrical and mechanical properties. Despite the availability of zinc, its poor corrosion resistance in acidic media has been a major challenge to its application (Odewunmi *et al.*, 2015). However, the use of corrosion inhibitors had been reported to be an efficient way of controlling its corrosion processes (Vashi and Prajapati, 2017). Most of the inhibitors used in the industries compose of some compounds that are toxic and have been presently facing a lot of criticisms due to their threat to human and their environments (Usman, 2017). The application of corrosion inhibitors is one among several corrosion protection methods. Recently, research activities have shifted grounds toward exploring of plant extracts as effective corrosion inhibitors due to environmental concerns of traditional organic and inorganic corrosion inhibitors. The efficacy of natural products extracted from different plant parts toward corrosion inhibition has been reported by several authors (Oguzie *et al.*, 2013 and Odewunmi *et al.*, 2015).

The use of natural products as corrosion inhibitors is in the fore front in the current trend of corrosion inhibition studies. The advocacy on the use of natural products as corrosion inhibitors

stemmed from the facts that they are cheap, renewable, readily available, ecologically acceptable and environmentally friendly moreover can be obtained by simple extraction procedures (El-Etre, 2016).

The main drawback of the use of plant extracts to appease the corrosion processes of metal in acidic media is the inability to point out the actual chemical component(s) that is/are responsible for its corrosion inhibition efficiency. The argument has been that plant extracts are comprised of mixtures of different organic compounds. However, the approach of isolating each component is very cumbersome and takes longer time for investigations. An alternative way that has been reported in the literature is to test the pure compounds of the identify principal/active component(s) together with the crude plant extract. For instance Garai *et al.* (2012) reported that Arbutin, an active principle from Artemisia pollens (*Asteraceae*) and the crude extract exhibited inhibition efficiency of 93% and 98% in 400 mg/L concentration at 30°C respectively for zinc in 1.0 M HCl solution.

MATERIALS AND METHODS

Metal sample collection and preparation

The analyzed zinc sheet used in the research had elemental compositions in percentage weight concentration as; (Zinc = 90.16 %, Carbon:

2.56 %, Oxygen: 2.36 %, Lead: 1.35 % and Copper 1.12 %). The zinc sheet was obtained from a fabrication workshop located in canteen area, Gusau, Zamfara State. The zinc sheet was mechanically press cut into coupons, each with an area of 2 cm x 2 cm, and a thickness of 0.02 cm, with a small hole near the upper edge of each specimen. Each coupon was abraded with emery paper of different grade grit size (GXX P60 and GXX P220). The residue particles from the polishing process were removed in ethanol bath for 10 minutes and dried in an open air after dipping in an acetone. The prepared zinc coupons were stored in the desiccator prior to use for corrosion studies (Fouda *et al.*, 2016; Nwosu and Muzaki, 2016).

Plant sample collection, identification, preparation and extraction

The watermelon fruit was obtained from a farm located along major fruit market road in Gusau, Zamfara state. The identification of the plant under study was carried out at the Herbarium section of the Department of Plant Biology, Bayero University, Kano with the Herbarium Accession Number (BUKHAN 0281; DPB/BUK/HIF/01026). The seeds were separated from the edible pulp, washed with running water followed rinsed with distilled water and sun dried for a period of two weeks. The seeds were heated at constant weight in an oven at 110°C for a period of 3 hours. About 500 g of the seeds were crushed to form powder using pestle and mortar and sieved using 250 nm mesh sieve. The finely powdered particles obtained were stored in plastic containers prior to extractions process (Chahul *et al.*, 2019a).

About 200 g weighed of finely powdered particles of watermelon seed was soaked in 1.5 litre of 99 % AR grade of ethanol for a period of two weeks with intermittent stirring. The solution was then filtered using Whatman No. 1 filter paper. The filtrate was concentrated in a rotary evaporator (RE52-3) between 40 – 50°C (Nwabanne and Okafor, 2012; Itodo *et al.*, 2018).

Preparation of solutions

The acid solution (0.1 M HNO₃) was prepared by accurately measuring 6.4 cm³ of HNO₃ (70%, 1.413 g/cm³). The acid was transferred drop by drop into 1000 cm³ volumetric flask containing about 250 – 300 cm³ of distilled water and filled up to the mark.

A 0.10% v/v concentration of WSE solution was prepared by measuring 1 cm³ of WSE and transferred into 1000 cm³ volumetric flask which containing about 250 – 300 cm³ of 0.1 M HNO₃ acid solution. After successful transfer, the 0.1 M HNO₃ acid solution was added and filled up to the mark. Other desired concentrations (0.02, 0.04, 0.06 and 0.08 %) were prepared.

Weight loss method

The weighed zinc coupons recorded as “W_i”, were tied with thread and completely immersed in 100 cm³ beaker which contained 50 cm³ of uninhibited and inhibited solutions of HNO₃ acid. The beakers were covered with aluminum foil to avoid particle from entering and to avoid evaporation of the corrosive media at high temperature. The zinc coupons were taken out after specific intervals, cleaned with hard brush in ethanol and air dried after dipping in acetone. The zinc coupons were then reweighed accurately and recorded as “W_f”. The weight losses “W_l” in the uninhibited and inhibited solutions are evaluated using equation 1. The triplicate experiment was carried out in each case and weight loss mean values of the zinc coupon were reported (Chahul *et al.*, 2019a).

$$W_l = W_i - W_f \quad (1)$$

The Corrosion rate C_R in (mg cm⁻² h⁻¹) of zinc coupon in uninhibited and in inhibited solutions, degree of surface coverage (θ) and inhibition efficiency (% I.E) were evaluated using equations 2, 3 and 4 respectively;

$$C_R = \frac{W_l}{At} \quad (2)$$

$$\theta = \frac{W_l^0 - W_l}{W_l^0} \quad (3)$$

$$\% I.E = \theta \times 100 \quad (4)$$

Where; W_l⁰ and W_l are the values of the average weight losses for the corrosion of zinc in the uninhibited and in inhibited solutions respectively, A is the area of zinc coupon in (cm²) and t is the time of immersion in (hour).

Effect of Immersion Time

The zinc coupons were separately immersed in 100 cm³ beakers containing 50 cm³ of uninhibited and inhibited solutions of 0.1 M HNO₃ acid at room temperature of 28 ± 1 °C and constant inhibitor concentrations of 0.02 %. The zinc coupons were removed from the solutions at time interval of 0.25, 0.5, 1.0, 1.5, 2.0, 2.5, 3.0 and 3.5 hours respectively (Chahul *et al.*, 2019b).

Effect of corrodent concentration

The prepared zinc coupons were weighed and immersed in 0.1, 0.2, 0.3, 0.4 and 0.5 M HNO₃ acid solutions at temperature of 28 ± 1 °C and constant inhibitor concentrations of 0.02 %. The final weights were taken and the average weight losses were recorded (Shakila *et al.*, 2017).

Effect of Inhibitor concentration and Temperature

The prepared zinc coupons were weighed and immersed in uninhibited and inhibited solutions of WSE with concentrations (0.02, 0.04, 0.06, 0.08 and 0.10 %) at different temperatures of 28, 35, 45 and 55 \pm 1 $^{\circ}$ C. The final weights were taken and the average weight losses were recorded. The concentrations of inhibitor with relatively higher inhibition efficiency were considered as the optimum concentrations (Odewunmi, 2015; Vashi and Prajapati, 2017; Vikas *et al.*, 2017).

Characterization

Fourier Transform Infrared Spectrophotometry (FT-IR) Analysis

FT-IR analyses were carried out using Agilent Technology, FT-IR (Cary 630) Fourier Transform Infrared Spectrophotometer. The corrosion products formed and WSE were subjected to FT-IR analysis by scanning it through the given wave number range of 4000 – 650 cm^{-1} .

Scanning Electron Microscopy

Surface morphologies of the zinc metal coupons were studied using (PRO: X: Phenom World 800-07334) model, manufactured by Phenom World Eindhoven, Netherlands. The scanned micrographs were taken at an accelerating voltage of 10.00 kV and x 300 magnification.

RESULTS AND DISCUSSION

Effect of Immersion Time

The results of corrosion rate and inhibition efficiency for corrosion of zinc in the uninhibited and inhibited solutions are presented in Figures 1 and 2 respectively. The results showed that the corrosion rates of zinc decreases with increase in immersion time at 28 \pm 1 $^{\circ}$ C. At the lowest immersion time of 0.25 hour, the corrosion rate of zinc in uninhibited and inhibited 0.1 M HNO_3 acid solutions were 26.0000 and 21.0000 $\text{mg cm}^{-2} \text{h}^{-1}$ respectively, while at the highest immersion time of 3.5 hours, the corrosion rates decreased to 6.0238 and 4.9071 $\text{mg cm}^{-2} \text{h}^{-1}$. This indicates that the more the contact time zinc is exposed to the corrosive environment the more the rate of dissolution will decrease.

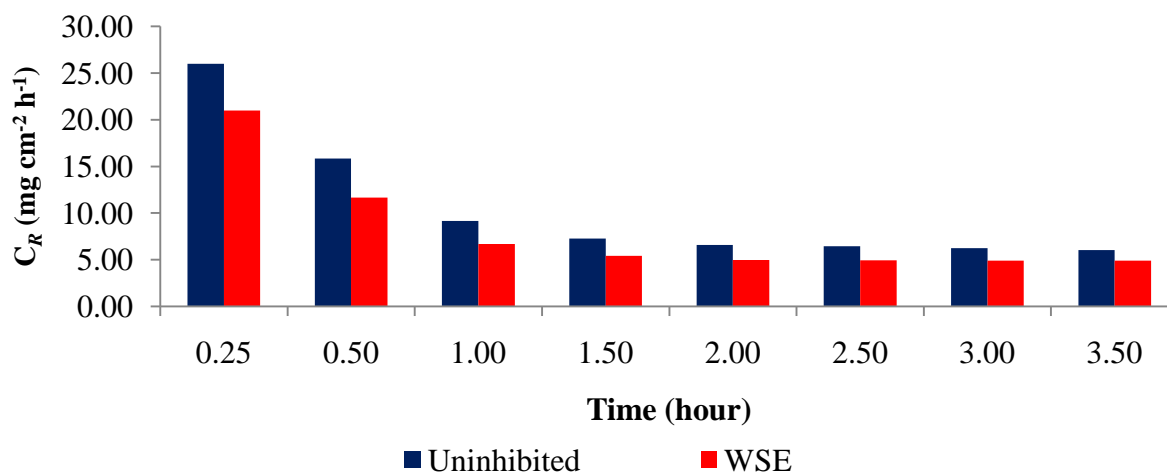


Fig. 1: Variation of Corrosion rate with immersion time

The non-linearity of corrosion rates of zinc plot in the uninhibited solution suggests that the zinc corrosion is a heterogeneous process involving several steps, similar results was reported by Usman (2017). Generally there was decrease in corrosion rates with time and this is due to the less

interactions that occur between the acid and the zinc surface in the solutions, which tend to destroy the metal surface gradually with time thereby decreasing the corrosion rate of the zinc, similar work was reported by Husaini *et al.* (2019).

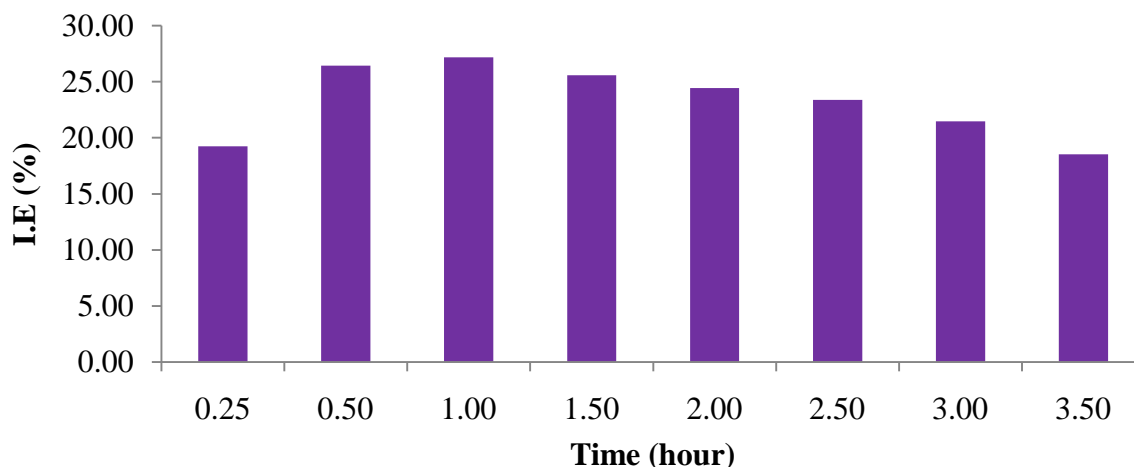


Fig. 2: Variation of inhibition efficiency with immersion time

The maximum inhibition efficiency observed in inhibited 0.02% WSE was 27.1825% at immersion time of 1 hour. Decrease in inhibition efficiency indicates the instability of protective film for the long time of immersion. Similar trend was reported by El-etre *et al.* (2016), who investigated the inhibition of acid aluminum corrosion in presence of aqueous extract of *domiana*.

Effect of Corrodent Concentration

The results presented in Figures 3 and 4 showed that, as the concentration of the acid increase the corrosion rate increases thereby decreases the inhibition efficiency, this is because rate of chemical reaction increases when the concentration of active species increase.

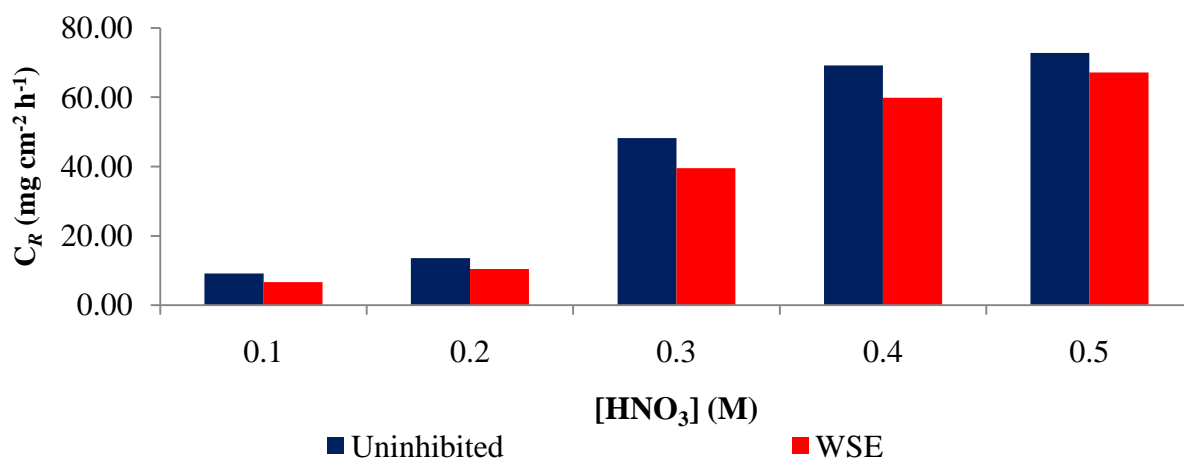


Fig. 3: Variation of Corrosion rate with Corrodent concentration

At the lowest used HNO₃ acid concentration of 0.1 M, the corrosion rates of zinc in a given uninhibited and inhibited 0.02% v/v WSE solutions were 9.1667 and 6.6750 mg cm⁻² h⁻¹, which corresponds to maximum corrosion inhibition efficiency of 27.1825%. While at the highest HNO₃ acid concentration of 0.5 M, the

corrosion rates increased to 72.7500 and 67.1250 mg cm⁻² h⁻¹ with inhibition efficiency of 7.7320%. This observation is due to the fact that chemical reaction increases as the concentration of the active species increases as reported by Shakila *et al.* (2017).

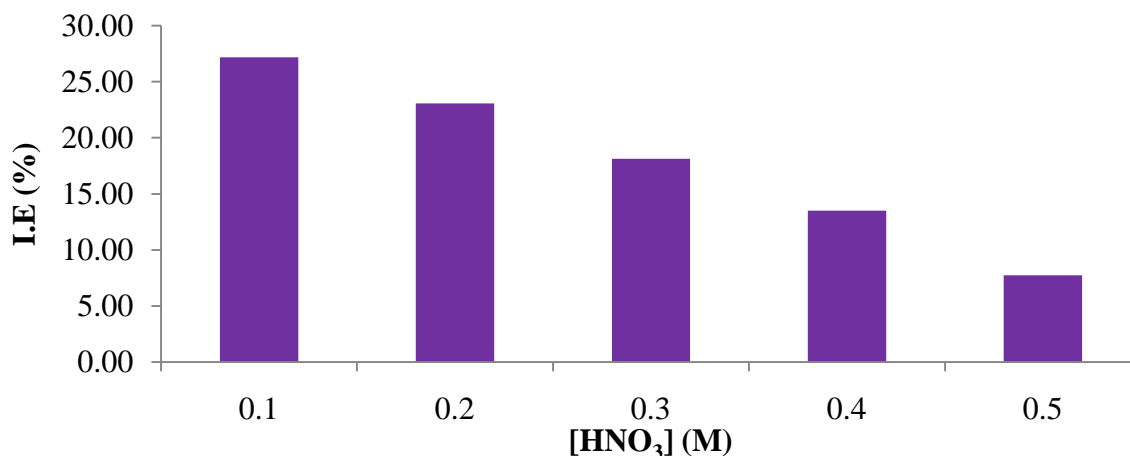


Fig. 4: Variation of inhibition efficiency with corrodent concentration

The dissolution rate of zinc depends on the concentration of the corrodent. This could be attributed to increase in concentration of the anions in the more concentrated acidic solution, which readily react with zinc ion present in the solution. Similar result was reported by Rathod and Vashi (2016), who investigated the effect of ammonium dichromate on the corrosion of aluminum in phosphoric acid and the result showed that the corrosion rate increased with increase in the concentration of the acid.

Effect of Inhibitor concentration and Temperature

The result in Figure 5, showed the variation of corrosion rate for the corrosion of zinc in the uninhibited and inhibited solutions at different WSE concentrations and temperatures. The results revealed that the corrosion rate was found to decrease with increasing concentrations of the WSE with corresponding increase in inhibition efficiency at constant temperature. On the other hand, the corrosion rate increases with increase in temperature at constant WSE concentrations with a resultant decrease in inhibition efficiency.

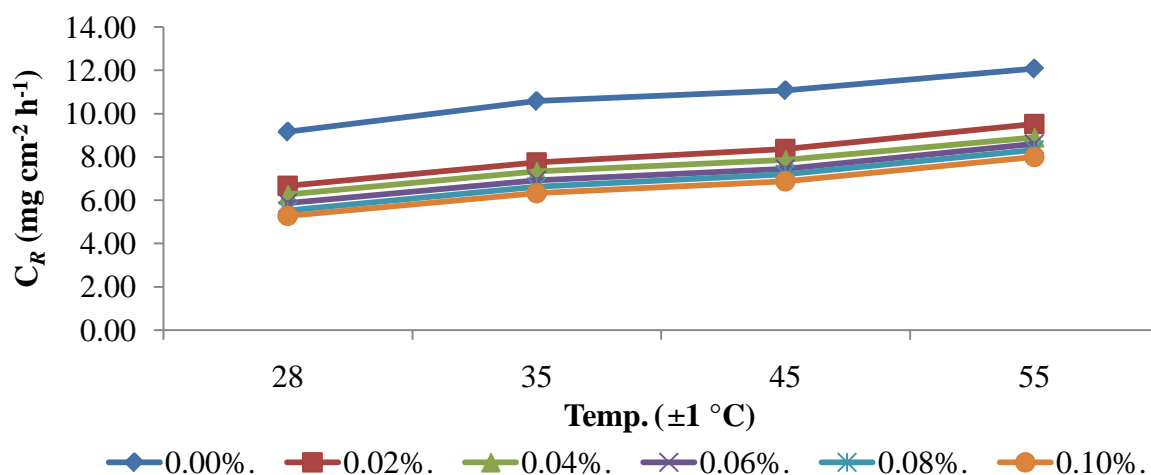


Fig. 5: Variation of Corrosion rate with Temperature and WSE concentration

At lowest used temperature of 28 ± 1 °C with the presence WSE concentrations of 0.00, 0.02, 0.04, 0.06, 0.08 and 0.10%, the corrosion rates of zinc were 9.1668, 6.6750, 6.2750, 5.8750, 5.5250, and 5.2750 $\text{mg cm}^{-2} \text{h}^{-1}$. With increasing the temperature to 55 ± 1 °C, the corrosion rate of zinc increased to 12.0833, 9.5250, 8.9000, 8.6000, 8.3250 and 8.0000 $\text{mg cm}^{-2} \text{h}^{-1}$. The values of corrosion rate of uninhibited system were found to

be higher when compared to the inhibited system. Examination of the result revealed that lowest corrosion rate was obtained at the highest concentration of the WSE. According to Vashi and Prajapati (2017), that corrosion rate is inversely proportional to the concentration of the inhibitor at constant temperature; similar phenomenon was observed in the present study. The corrosion rate in the presence of inhibitor was reduced indicating the

inhibiting action of the compounds presence in the inhibitor. This suggests that as the concentration of WSE increases, there is an increase in surface coverage of the adsorbed molecules on the zinc surface which provided a barrier (film) and reduced further corrosion, the same scenario was reported by Vikas *et al.* (2017). Furthermore, similar results were reported by Odewunmi *et al.* (2015), who carried out research on Utilization of watermelon rind extract (WMRE) as corrosion inhibitor for mild steel in acidic media.

It can be observed from the results that the highest corrosion rate of zinc was observed at the highest temperature (55 ± 1 °C). This observation is

due to the fact that chemical reaction rates generally increases with rising temperature. Increase in temperature leads to increase in the kinetic energy possessed by the reacting molecules thereby making the molecules to overcome the energy barrier faster as reported by El-etre *et al.* (2016) and Vikas *et al.* (2017).

Furthermore, the result in Figure 6, showed that the inhibition efficiency decreases with increase in temperature. The inhibition efficiency for the corrosion of zinc at 28 ± 1 °C in the presence of WSE concentrations 0.02, 0.04, 0.06, 0.08 and 0.10% v/v were 27.1825, 31.5461, 35.9097, 39.7278 and 42.4551 %.

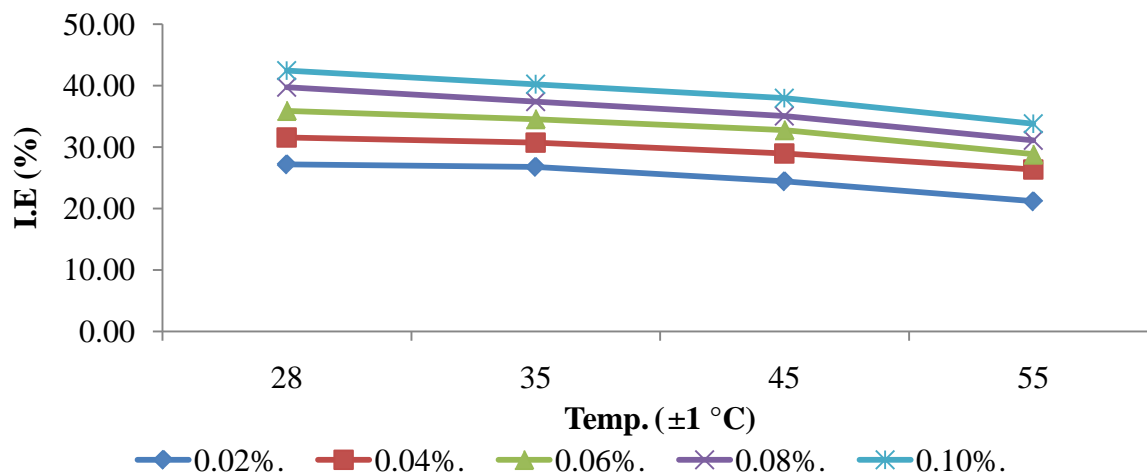


Fig. 6: Variation of inhibition efficiency with Temperature and WSE concentration

With increasing the temperature to 55 ± 1 °C, the inhibition efficiency reduced to 21.1724, 26.3448, 28.8276, 31.1034 and 33.7931 %. The decrease in inhibition efficiency as temperature increases in a given constant WSE concentrations could be attributed to desorption of WSE compounds that were already adsorbed on zinc surface by electrostatic attraction. Similar work was reported by James and Akaranta (2014) while investigating the corrosion inhibition of Aluminum in 2.0 M Sulphuric acid using Acetone extract of red Onion skin, the result of the inhibition efficiency was found to decrease with increase in temperature

Adsorption study

To investigate surface coverage and best fit model, the experimental data were tested with five adsorption isotherm models (Langmuir, Freundlich, Frumkin, Temkin and Flory-Huggins adsorption). The WSE concentrations (C_{inh}), corrosion rates (C_R) and degrees of surface coverage (θ) were used in testing different adsorption isotherm models and subsequently evaluated adsorption parameters and equilibrium constant (K_{ads}).

Langmuir adsorption isotherm is expressed according to equation 5.

$$\frac{C_{inh}}{\theta} = \frac{1}{K_{ads}} + C_{inh} \quad (5)$$

Where, C_{inh} is the concentration of the WSE, θ is the degree of surface coverage, K_{ads} is the adsorption equilibrium constant.

Equation 6 is obtained by taking the logarithm of both sides of equation 5 (Nwabanne and Okafor, 2012).

$$\log \left(\frac{C_{inh}}{\theta} \right) = \log C_{inh} - \log K_{ads} \quad (6)$$

Plot of $\log \frac{C_{inh}}{\theta}$ versus $\log C_{inh}$ will produce a straight line with intercept equals to $-\log K_{ads}$ with slope of almost unity.

Freundlich adsorption isotherm is expressed in equation 7.

$$\log \theta = n \log C_{inh} + \log K_{ads} \quad (7)$$

Where, n is an adsorption parameter such that $0 \leq n \leq 1$. Plot of $\log \theta$ against $\log C_{inh}$ gives linear plot (Hussaini *et al.*, 2019).

The Frumkin adsorption isotherm is given by equation 8.

$$\log \left\{ C_{inh} \left[\frac{\theta}{1-\theta} \right] \right\} = 2.303 \log K_{ads} + 2\alpha\theta \quad (8)$$

$$\theta = \frac{-2.303 \log K_{ads}}{2\alpha} - \frac{2.303 \log C_{inh}}{2\alpha} \quad (10)$$

Where, α is the lateral interaction term describing the interaction in the adsorbed layer. Plots of $\log \left\{ C_{inh} \left[\frac{\theta}{1-\theta} \right] \right\}$ versus θ give linear plot with intercept equals to $2.303 \log K_{ads}$ which shows the applicability of Frumkin isotherm (Akinbulumo *et al.*, 2020).

In Temkin adsorption isotherm, the degree of surface coverage (θ) is related to inhibitor concentration (C_{inh}) according to equation 9 (Akinbulumo *et al.*, 2020).

$$\exp(-2\alpha\theta) = K_{ads} x C_{inh} \quad (9)$$

Where, α is the attractive parameter. Rearranging and taking logarithm of both sides of equation 9 gives equation 10.

Plot of θ against $\log C_{inh}$ gives a linear relationship.

Flory-Huggins adsorption isotherm is expressed according to equation 11.

$$\log \left(\frac{\theta}{C_{inh}} \right) = \log K_{ads} + x \log (1 - \theta) \quad (11)$$

Where, x is the size parameter and is a measure of the number of adsorbed water molecules substituted by a given inhibitor molecule. The plot of $\log \left(\frac{\theta}{C_{inh}} \right)$ against $\log (1 - \theta)$ gives linear relationship with intercept equals to $\log K_{ads}$ (Chandrabhan *et al.*, 2018).

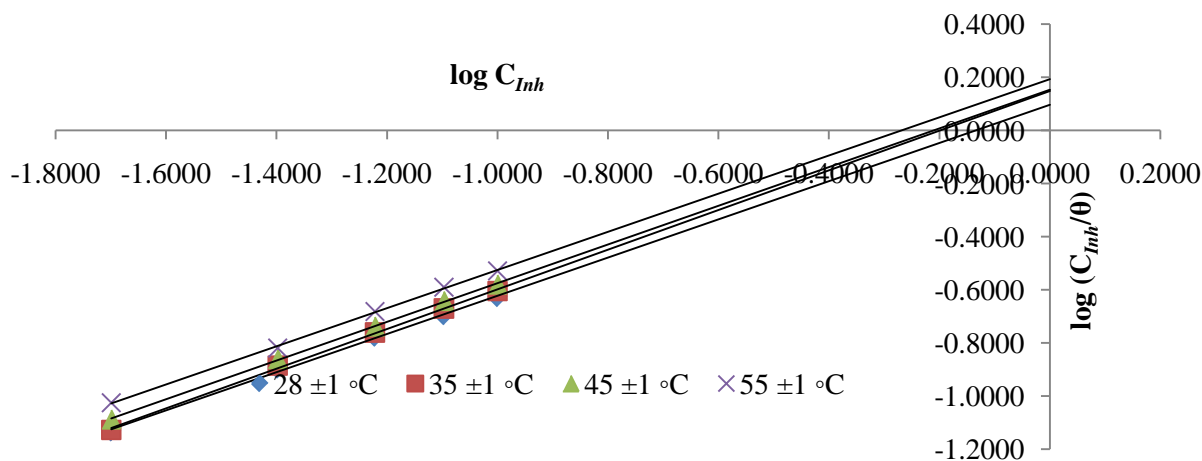


Fig. 7: Langmuir isotherm plot

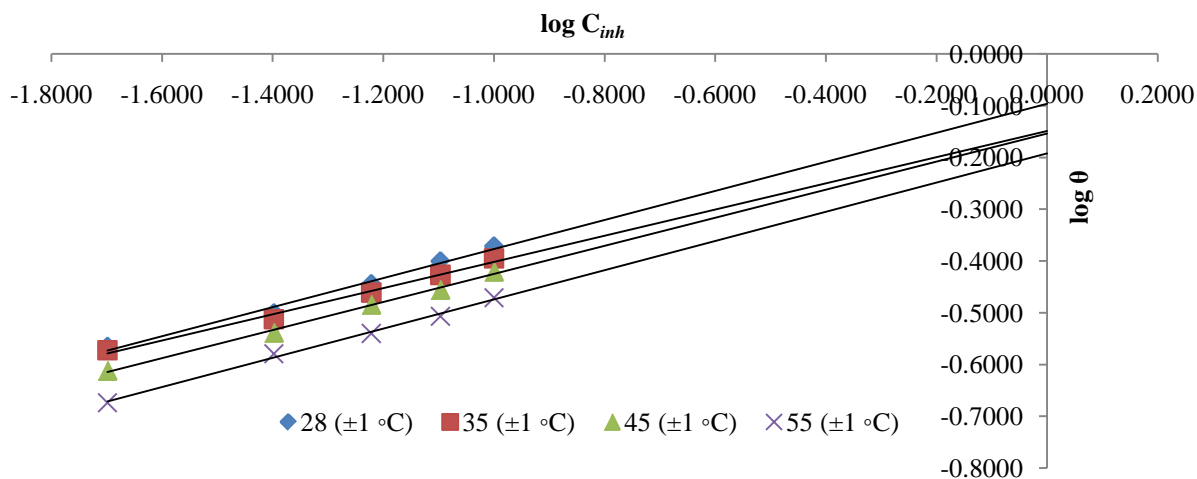


Fig. 8: Freundlich isotherm plot

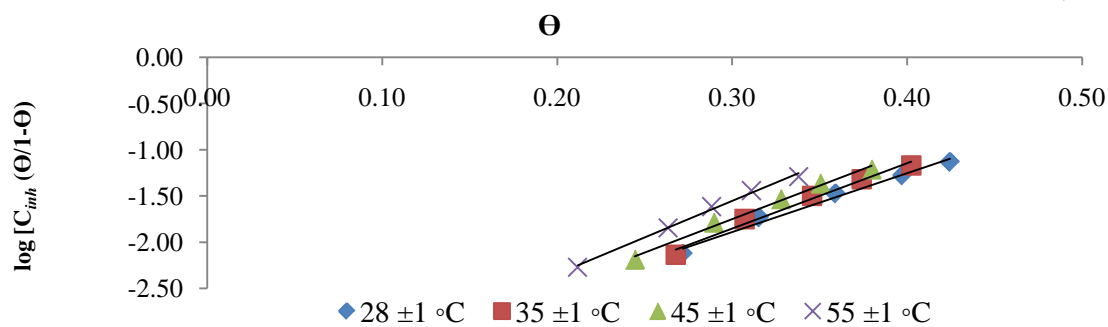


Fig. 9: Frumkin isotherm plot

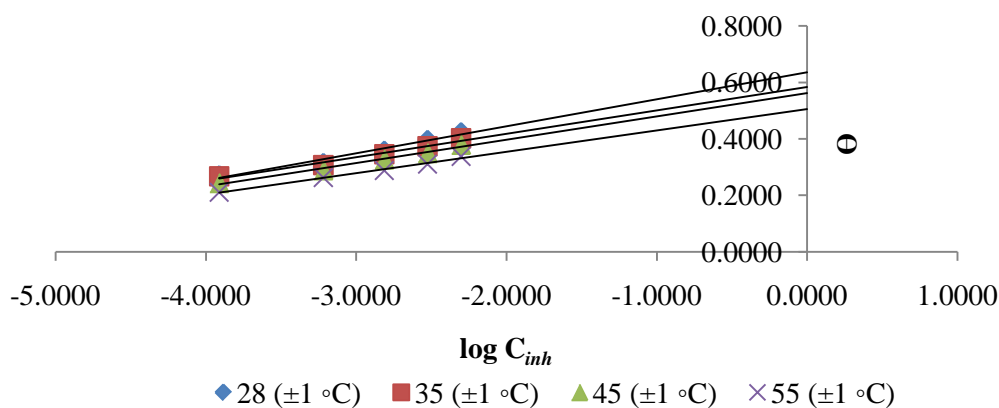


Fig. 10: Temkin isotherm plot

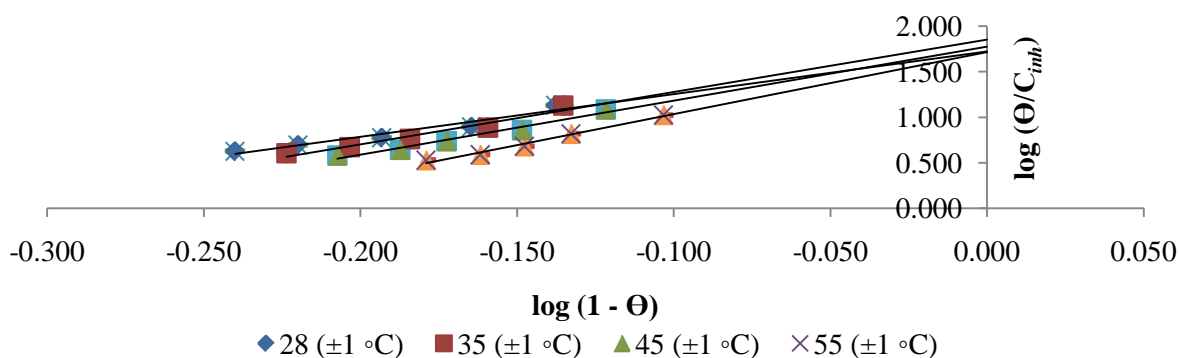


Fig. 11: Flurry-Huggins isotherm plot

The efficiency of a compound as a successful inhibitor is mainly dependent on its ability to get adsorbed on the metal surface, which consists of the replacement of water molecules at the corroding interface (Chandrabhan *et al.*, 2018; Husaini *et al.*, 2019). To ascertain the nature of adsorption, the surface coverage values for the inhibitors obtained from weight loss measurement were theoretically fitted into five different isotherm models namely; Langmuir, Freundlich, Frumkin, Temkin and Flory-Huggins adsorption isotherm

using equations 6 - 11. Their regression coefficient (R^2) and adsorption parameters were used to determine the best fit isotherm among them.

The results presented in Table 1, shows the adsorption parameters of linearization of each of the isotherm models. The data fitted the models taking into consideration the values of regression coefficient (R^2) close to unity (Sulaiman, 2017). All the tested models gave good linearity, with the Langmuir model having the best fit.

Table 1: Adsorption isotherm parameters

Temp. (K)	Langmuir		Freundlich		Temkin		Frumkin		Flory-Huggins	
	R ²	R _L	R ²	N	R ²	α	R ²	α	R ²	b
301	0.998	0.984	0.988	0.280	0.984	-3.181	0.973	5.263	0.945	4.696
308	0.998	0.986	0.990	0.253	0.985	-3.539	0.975	6.098	0.953	5.764
318	0.999	0.986	0.996	0.271	0.991	-3.616	0.986	6.098	0.973	5.934
328	0.999	0.987	0.995	0.282	0.994	-3.957	0.991	6.667	0.983	6.804

The essential characteristic of Langmuir isotherm can be expressed in term of a dimensionless separation factor (R_L). Value of R_L<1 indicates a favorable adsorption, R_L> 1 unfavorable adsorption, R_L = 1 linear and R_L = 0 irreversible. Generally, 0 <R_L< 1 is sign of favorable adsorption (Husaini *et al.*, 2019). The calculated values of R_L are all greater than zero but less than unity as indicated in Table 1, hence this implied favorable adsorption. The adherence of the inhibitor molecules may partially occur with monolayer adsorption onto a homogenous surface containing a finite number of identical sites and absence of lateral interactions between the adsorbed species.

Adsorption equilibrium constant

As shown in Table 2 the adsorption equilibrium constants obtained at various temperatures were evaluated from the intercept of the Langmuir plot. The adsorption equilibrium constants, K_{ads} values are all positive, indicating the feasibility of the adsorption of the WSE to the zinc metal surface. The adsorption equilibrium constant decreases with increase in temperature. According to Hegazy (Chandrabhan *et al.*, 2018), this indicates that at a higher temperature, the adsorbed WSE tends to desorbs back from the zinc surface.

Table 2: Thermodynamic parameters

Temperature (K)	K _{ads}	ΔG _{ads} (kJ/mol)	ΔH _{ads} (kJ/mol)	ΔS _{ads} (kJ/mol)
301	0.8017	-9.4996	-0.5533	29.7220
308	0.7096	-9.4080	-0.8787	27.6924
318	0.7031	-9.6891	-0.9316	27.5392
328	0.6427	-9.7488	-1.2058	26.0457

Thermodynamic study

Generally, the values of ΔG_{ads} around -20 kJmol⁻¹ are consistent with electrostatic interaction between charged molecules and charged metal which indicate physisorption, while those above -40 kJmol⁻¹ involved charge sharing or transfer from the inhibitor molecule to the metal surface to form a coordinate type of bond which indicates chemisorption (Odewunmi *et al.*, 2015, Chahul *et al.*, 2019a). As shown in the Table 2, the ΔG_{ads} values are all less than -20 kJ/mol. This result indicates that adsorption of the WSE on zinc surface is spontaneous, feasible and occurred according to the mechanism of physical adsorption. The values of ΔH_{ads} are all negative, this indicating the exothermic nature of the reaction process; also suggest that the higher temperature favors the corrosion process (Nwabanne, 2012).

Basically, ΔH_{ads} positive values up to 40 kJmol⁻¹ are related to physisorption while those around 100 kJmol⁻¹ or higher are attributed to chemisorption while ΔH_{ads} negative values could be attributed to both physisorption and chemisorption processes (Rathod and Vashi, 2016). The decrease in ΔS_{ads} with increase in temperature implies there is a reduction in the entropy i.e., decrease in spontaneity and stability of the adsorption at a higher temperature (Awe *et al.*, 2015)

Characterization

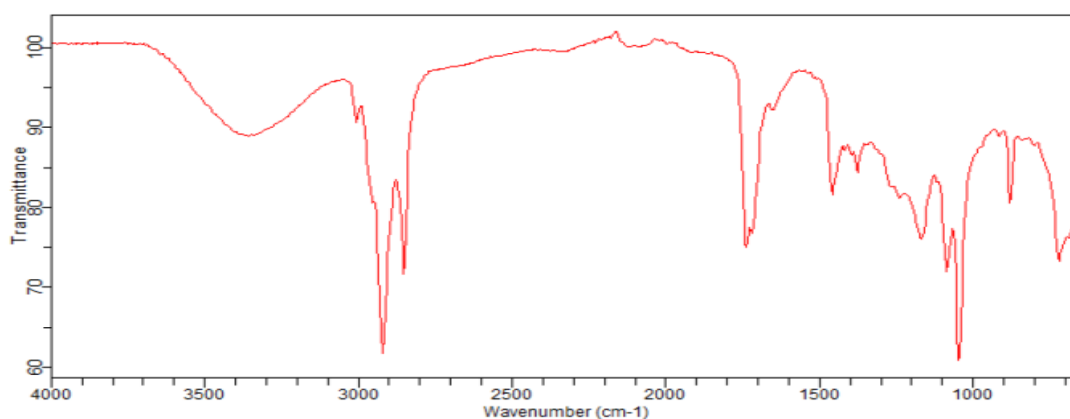
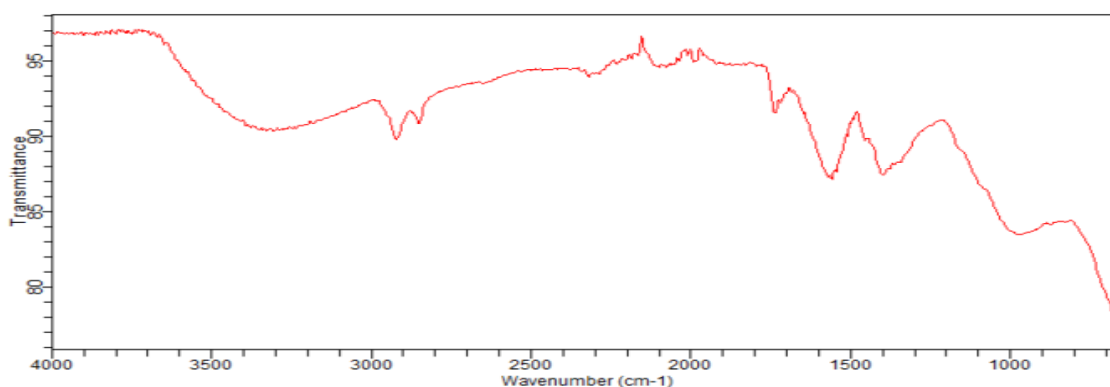
The FT-IR spectra of WSE and corrosion product in inhibited 0.10 % v/v solution are presented in Figures 12 and 13 respectively. Also, the peak values extracted from the spectra are presented in Table 3.

Table 3: FT-IR peak values for WSE and corrosion product in inhibited 0.10 % v/v solution

Functional groups	WSE peak values (cm ⁻¹)	Corrosion product peak values (cm ⁻¹)
O-H stretch (3570–3200 cm ⁻¹ broad)	3357	3379
C=C vibration (1750–1725 cm ⁻¹)	1741	1737
C=O vibration (1725–1700 cm ⁻¹)	1722	1718
C=N stretching vibration (1680–1630 cm ⁻¹)	1652	1645

It has been observed that most of the functional group present in the WSE spectrum was also noticed in the spectrum of corrosion product though with different intensity. This confirms the fact that the WSE compounds were actually adsorbed on the zinc surface through the

mechanism of physical adsorption. The shift and the change in adsorption bands observed in the stretching frequencies suggest that the functional group present in the WSE compounds bind to the zinc surface.

**Fig. 12: FT-IR spectrum of WSE****Fig. 13: FT-IR spectrum of zinc corrosion product in the inhibited 0.10% v/v of WSE**

Scanning Electron Microscopic images of zinc samples were presented in Figures 14a-c. Figure 14a present the micrograph of zinc sample after polishing prior to use in corrosion study. Figure 14b shows the surface morphology of zinc sample immersed in uninhibited 0.1 M HNO₃ acid, the surface was very rough, cracks, patches, pores and highly damaged due to the attack of the aggressive acid while Figure 14c revealed how the zinc surface was prevented from HNO₃ acid attack

by the presence of 0.10 % of WSE. It can be deduced that the WSE used had inhibited zinc dissolution in acid by covering the surface area with protective film which was found absent in case of acid interaction with zinc in uninhibited solution. This observation from the micrographs has very close correlation with the results obtained from the weight loss method. This clearly proved that the inhibition is due to the formation of an adsorbed film through the process of adsorption of the WSE compounds on the zinc surface.

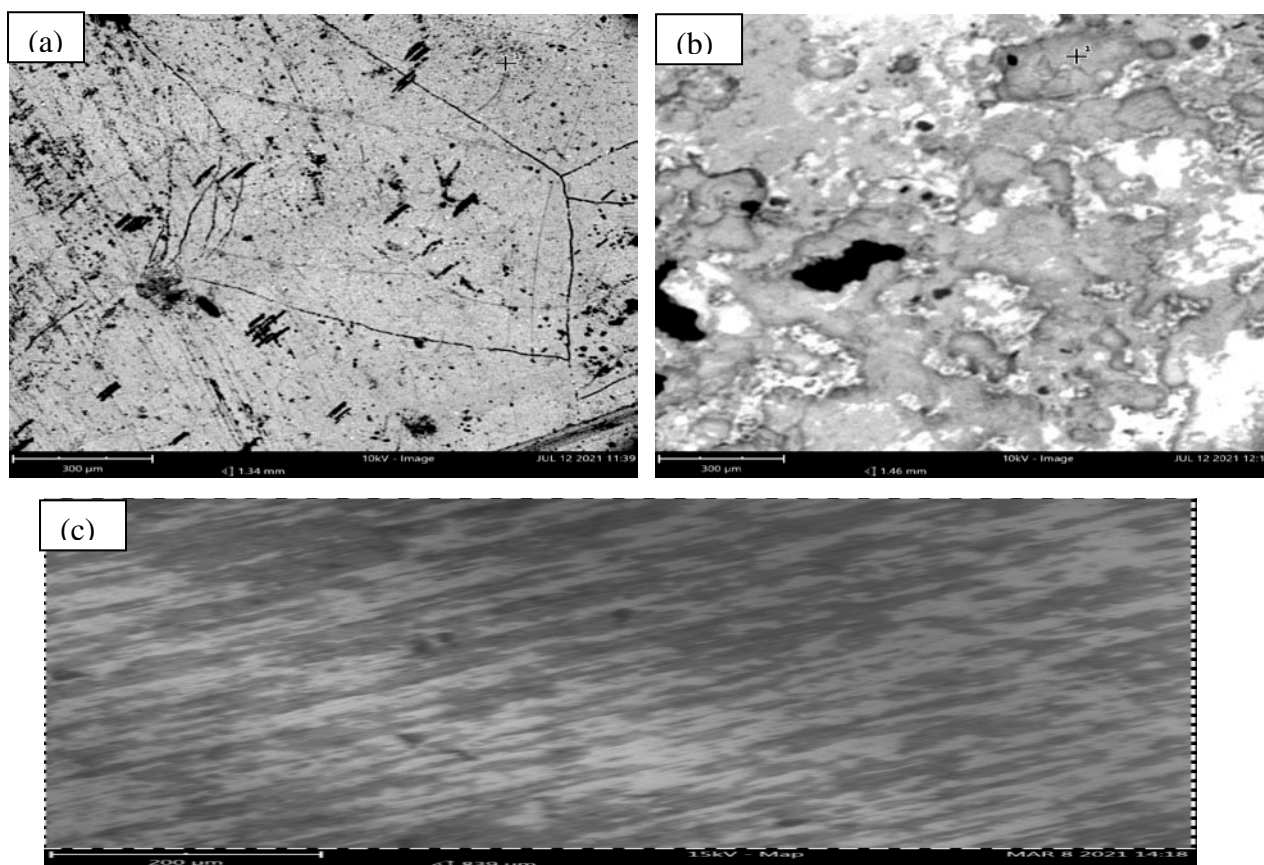


Fig. 9: Micrographs of (a) un-reacted zinc sample (b) reacted zinc sample in the uninhibited HNO_3 solution (c) reacted zinc sample in the inhibited 0.10% v/v of WSE.

CONCLUSION

The results obtained from weight loss method showed that the inhibition efficiency increases with increase of the concentration of the WSE also decreases with increase in temperature. The adsorption isotherm model is best fitted to Langmuir isotherm model. The adsorption process indicated feasible and spontaneous process from the large negative values of ΔG_{ads} . The values of ΔH_{ads} are all negative indicating exothermic process of adsorption.

REFERENCES

- Akinbulumo Olatunde Alaba, Oludare Johnson Odejobi, Ebenezer Leke Odekanle (2020). Thermodynamics and adsorption study of the corrosion inhibition of mild steel by *Euphorbia heterophylla* L. extract in 1.5 M HCl, *Materials* 5, 100074 <https://doi.org/10.1016/j.rinma.2020.100074>
- Awe F.E, Idris S.O, Abdulwahab M, Oguzie E. E., (2015). Theoretical and experimental inhibitive properties of mild steel in HCl by ethanol extract of *Boscia senegalensis*. *Cogent Chemistry*, 7(9): 12676.
- Chahul, H. F., Ndukwe, G. I., Ladan, A. A. (2019a). Adsorption Behaviour and Corrosion Inhibition Effect of *N. imperialis p.beauv (Lecythidaceae)* Seed Extract on Mild Steel in 1.0 M HCl, *ChemSearch Journal* 10(1): 25 – 32.
- Chahul H. F., Danat B. T., Maji, E. (2019b). Corrosion Inhibition Performance of Ethanol Extract Leaves of *Cucurbita pepo* (Pumpkin) on Mild Steel in Acidic Media, *ChemSearch Journal* 10(1): 46 – 53.
- Chandrabhan Verma, Eno E. Ebenso, Indra Bahadur, M.A. Quraishi (2018). An overview on plant extracts as environmental sustainable and green corrosion inhibitors for metals and alloys in aggressive corrosive media, *Journal of Molecular Liquids* 266, 577–590, journal homepage: www.elsevier.com/locate/molliq
- El-Etre A. Y., Shahera M. Shohayeb, M. A. Elkomy, S. Abdelhamed (2016). Inhibition of Acid Aluminium Corrosion in Presence of Aqueous Extract of Domiana, *Journal of Basic and Environmental Sciences*, 3, 25 – 36.
- Fouda, A. S., M. Morsi, H. A. Mosallam (2016). *Capsicum* extract as green corrosion extract for carbon steel in hydrochloric acid solutions, “*Zastita Materijala*”, 57 (1) 33 - 45.
- Garai S., Jaisankar P., Singh J. K., Elango A. (2012). A comprehensive study on crude methanolic extract of *Artemisia pollens*

- (*Asteraceae*) and its active component as effective corrosion inhibitors of mild steel in acidic solution, “*Corrosion Science*, 60, 193 – 204.
- Husaini, M. Usman, B., Ibrahim, M. B. (2019). Adsorption and characterization of anisaldehyde as corrosion inhibitor for Aluminum corrosion in hydrochloric acidic environment, *i-manager’s Journal on Chemical Sciences*, 1(1): 36 – 45.
- Itodo A.U., Aondofa B.G., Iorungwa M.S. (2018). Retarding Mild Steel Corrosion using a Blend of Schiff Base Metal Complex and Neem Plant Extract, *ChemSearch Journal* 9(2): 45 – 63.
- James, A. O., O. Akaranta, (2014). Corrosion Inhibition of Aluminium in 2.0 M Sulphuric acid using Acetone extract of red Onion skin, *International Journal of Applied Chemical Sciences Research*, 2(1): 1 – 10. <http://ijacsr.com/>
- Nwabanne Joseph Tagbo, Vincent Nwoye Okafor (2012). Adsorption and Thermodynamics Study of the Inhibition of Corrosion of Mild Steel in H₂SO₄ Medium Using *Vernonia amygdalina*, *Journal of Minerals and Materials Characterization and Engineering*, 11, 885-890.
- Nwosu, F. O., Muzakir, M. M. (2016). Thermodynamic and Adsorption studies of corrosion inhibition of mild steel using lignin from siam weed (*Chromolaena odorata*) in acid medium, “*J. Mater. Environ. Sci.*”, 7 (5) 1663-1673.
- Odewunmi, Nurudeen A., Saviour A. Umoren, Zuhair M. Gasem, Saheed. A. Ganiyu, Qamaruddin Muhammad, (2015). 1-Citrulline: An active corrosion inhibitor component of watermelon rind extract for mild steel in HCl medium, *Journal of the Taiwan Institute of Chemical Engineers*, 51, 177 – 185. www.elsevier.com/locate/jtice
- Oguzie, E. E., Oguzie K. L., Akalezi C. O., Udeze I. O., Ogbulie J. N., Njoku V. O. (2013). Natural products for materials protection: corrosion and microbial growth inhibition using *Capsicum frutescent* biomass extracts, “*ACS Sustainable Chem. Eng.*”, 2013:1:214–25.
- Rathod, K. N., Vashi, R. T., (2016). Inhibition effect of ammonium dichromate on the corrosion of aluminum in phosphoric acid, “*International Journal of Chemical Studies*” 4 (1), 37 -42.
- Shakila, D., K. Veni, A. Dinesh Karthik, K. Geetha (2017). Green Synthesis, Characterizations, Corrosion Inhibition and Biological Applications of Schiff Base Transition Metal Complexes, *IOSR Journal of Pharmacy*, 4(2):62 - 68. www.iosrphr.org
- Sulaiman, Zakariyau (2017). Comparative studies on the Corrosion Inhibition of Tin in Acidic and Alkaline media using Henna leaves powder and Caffeine as Inhibitors. M.Sc. thesis, Department of Pure and Industrial Chemistry, Bayero University, Kano.
- Usman, Sani Abdul (2017). Corrosion Inhibition potential of the fruits Gmelina aborea (Juice) and Acacia (Powder and Ethanol extract) on Aluminum, M.Sc. thesis, Department of Pure and Industrial Chemistry, Bayero University, Kano.
- Vashi, R.T., N. I. Prajapati, (2017). Corrosion Inhibition of Aluminum in Hydrochloric Acid using *Bacopa monnieri* leaves extract as green inhibitor, *International Journal of Chem. Tech. Research*, 10 (15): 221 - 231.
- Vikas, Hari Om, Anjoo Bala, Pradeep Kumar, (2017). Isatin Schiff Base as an Eco friendly Corrosion Inhibitor for Carbon Steel in 1.0 M HCl, *Der Pharma Chemica*, 9 (12): 92 - 99 <http://www.derpharmachemica.com/archives.html>.